



***Chlamydia trachomatis* Glyceraldehyde 3-phosphate dehydrogenase:
Enzyme Kinetics, High Resolution Crystal Structure and Plasminogen**

Binding

Norbert Schormann¹, Juan Campos², Rachael Motamed², Katherine L. Hayden², Joseph R. Gould³, Todd J. Green³, Olga Senkovich⁴, Surajit Banerjee⁵, Glen C. Ulett⁶ and Debasish Chattopadhyay^{7*}

¹Department of Biochemistry, University of Alabama at Birmingham, Birmingham, AL, USA

²Department of Chemistry and Physics, Birmingham-Southern College, Birmingham, AL, USA

³Department of Microbiology, University of Alabama at Birmingham, Birmingham, AL, USA

⁴Department of Biochemistry and Molecular Genetics, Midwestern University, Glendale, AZ, USA

⁵Northeastern Collaborative Access Team and Department of Chemistry and Chemical Biology, Cornell University, Argonne, USA

⁶School of Medical Sciences, and Menzies Health Institute Queensland, Griffith University, Parklands, Australia

⁷Department of Medicine, University of Alabama at Birmingham, Birmingham, AL, USA

This article has been accepted for publication and undergone full peer review but has not been through the copyediting, typesetting, pagination and proofreading process which may lead to differences between this version and the Version of Record. Please cite this article as doi: 10.1002/pro.3975

*Correspondence: dchatop@uabmc.edu Phone: +1 205934124

ABSTRACT

Glyceraldehyde 3-phosphate dehydrogenase (GAPDH) is an evolutionarily conserved essential enzyme in the glycolytic pathway. GAPDH is also involved in a wide spectrum of non-catalytic cellular ‘moonlighting’ functions. Bacterial surface-associated GAPDHs engage in many host interactions that aid in colonization, pathogenesis and virulence. We have structurally and functionally characterized the recombinant GAPDH of the obligate intracellular-bacteria *Chlamydia trachomatis*, the leading cause of sexually transmitted bacterial and ocular infections. Contrary to earlier speculations, recent data confirm the presence of glucose-catabolizing enzymes including GAPDH in both stages of the biphasic life cycle of the bacterium. The high resolution crystal structure described here provides a close-up view of the enzyme’s active site and surface topology and reveals two chemically modified cysteine residues. Moreover, we show for the first time that purified *C. trachomatis* GAPDH binds to human plasminogen and plasmin. Based on the versatility of GAPDH’s functions data presented here emphasize the need for investigating the *Chlamydiae* GAPDH’s involvement in biological functions beyond energy metabolism.

KEYWORDS

Chlamydia, GAPDH, plasminogen binding, plasmin binding, enzyme kinetics, reactive cysteine, crystal structure, glycolysis, STD/STI, protein-protein interaction

INTRODUCTION

Chlamydia trachomatis (*Ct*) is an obligate intracellular pathogen of eukaryotic cells. *Ct* is a major cause of sexually transmitted bacterial infections worldwide and a leading cause of preventable blindness in the developed world.^{1,2} Chronic *Chlamydiae* infection in women can lead to serious long-term diseases including cervical and uterine cancers.^{2,3} Although treatable by antibiotics, treatment failure and reinfections hamper *Chlamydiae* control in developed countries.^{4,5} New targets for developing drugs and a vaccine are urgently needed. However, there is a critical gap in our understanding of the biochemical pathways and potential therapeutic targets.

Chlamydiae have a unique biphasic life cycle alternating between infectious extracellular elementary bodies (EBs) and intracellular replicative reticulate bodies (RBs). Although historically *Chlamydiae* are considered an 'energy parasite', bacterial enzymes for glycolysis (except hexokinase), the tricarboxylic acid cycle and pentose phosphate pathway have been identified in both life stages.^{1,6} Among the most expressed glycolytic enzymes is Glyceraldehyde 3-phosphate dehydrogenase (GAPDH).¹ This tetrameric essential enzyme catalyzes the reversible oxidative phosphorylation of D-glyceraldehyde 3-phosphate (D-G3P) into 1,3-diphosphoglycerate using NAD⁺ as cofactor and plays a key role in cellular metabolism by generating NADH. Due to its indispensable role in glycolysis GAPDH enzyme activity is a potential drug target.⁷

Accepted Article

Additionally, GAPDHs participate in a wide range of catalysis-independent cellular functions that are coined ‘moonlighting activities’.⁸ Although predominantly a cytoplasmic protein GAPDHs associated with microbial surfaces facilitate host-pathogen interactions, colonization, pathogenesis and immunomodulation.⁹⁻¹³ Bacterial surface resident GAPDHs bind to various host macromolecules including fibronectin, plasminogen and complement proteins, and are implicated in host cell invasion and immune evasion.¹⁴⁻¹⁸ The moonlighting functions may also be potentially useful therapeutic targets.¹⁹ Moreover, Group B Streptococcus GAPDH (*GBSGAPDH*) is proposed as a potential vaccine candidate.²⁰ Interestingly, GAPDH was found to be one of the T-cell antigens purified from mice infected with *C. muridarum* (*Cm*).²¹

The presence of GAPDH in both EBs and RBs underscores its importance throughout the bacterial life cycle. Active GAPDH enzyme was found in the RB extract but the kinetic parameters have not been determined. As part of our studies on microbial GAPDHs, we have expressed, purified and characterized recombinant *Ct* GAPDH (*CtGAPDH*) structurally and functionally. We describe here the high resolution crystal structure of the holo enzyme refined at 1.5 Å resolution. The structure displays two chemically modified cysteine residues. Furthermore, we report for the first time that *CtGAPDH* binds to human plasminogen (hPIg) and human plasmin (hPln) *in vitro*.

RESULTS AND DISCUSSION

Enzyme activity optimization and kinetics

The optimum pH for *CtGAPDH* activity was 9.0 [Fig. 1(A)]. The optimum pH of GAPDH enzymes from many organisms is between 7.5-9.5 with the majority exhibiting highest activity in

the pH range of 8.5-9.5.^{9,22-26} Values of K_M for NAD^+ and D-G3P calculated from the Michaelis-Menten (M-M) plots were 0.139 (0.016) mM and 0.611 (0.089) mM respectively, and the value of V_{\max} was 49.6 (1.84) $\mu\text{M NADH min}^{-1} \text{mg}^{-1}$ [Fig. 1(B), 1(C)]. In Table 1 we compare the M-M parameters for *Ct*GAPDH with those of other GAPDH enzymes. These parameters for GAPDHs from different organisms vary widely. It should be noted that the reported values are often based on experiments performed at pHs different from the optimum pH. The kinetics parameters (K_M for NAD^+ and D-G3P, and the V_{\max}) of *Ct*GAPDH are very similar to those of *Mycobacterium tuberculosis* GAPDH.²⁵ The K_M for NAD^+ is also similar to the values reported for GAPDHs of Group A *Streptococcus*⁹ and *B. stearothermophilus* (measured at optimum pH).²⁶ The K_M value for D-G3P of *Ct*GAPDH is closer to those of the bacterial counterparts than enzymes from eukaryotes.

Overall structure quality

*Ct*GAPDH crystallized in space group $P2_1$ as a tetramer in the asymmetric unit with subunits (A, B, C and D) related by 222 non-crystallographic symmetry (Fig. 2). The crystal structure was refined to 1.5 Å resolution. Due to insufficient electron density the C-terminal residue Lys334 (all subunits) and one other residue (Val100 in subunits B and C) were not modelled. The overall quality of the structures is excellent (Table 2) with only one outlier, Val238. Val238 is in a well-defined loop linking adjacent antiparallel β -strands. The atypical backbone geometry is stabilized by a hydrogen bond between the peptide nitrogen atom of Val238 and Asn314 as observed in other GAPDH structures.^{24,27} The root mean square deviation (*rmsd*) of bond distances (0.013 Å) and

bond angles (1.69°) indicate excellent geometry. Recently, the 2.4 Å resolution structure of *Ct*GAPDH in space group $P2_12_12_1$ was reported.²⁸ Our high resolution structure is similar to the reported structure (*6OK4*) with an *rmsd* of 0.29 Å for superposition of the tetramers but reveals additional features not noted in *6OK4*.

***Ct*GAPDH tetramer assembly**

The *Ct*GAPDH tetramer consists of dimers AB and CD, and exhibits two major and one minor interfaces (Fig. 2). The major interface P is contributed by subunits A, B and C, D with the dimer interfaces formed by 108 residues spanning across 3741 Å² and 3767 Å² of buried surface area, respectively. The second largest interface Q is generated by subunit pairs A, C and B, D with 72 and 74 residues contributing to 2805 and 2846 Å² of interface area (buried surface area), respectively. GAPDHs display an evolutionarily conserved three-dimensional (3D) structure and topology. Figure S1 shows a structure-based alignment of GAPDH sequences from selected organisms. Each GAPDH subunit folds into two domains: the cofactor-binding domain (residues 1-150, 314-334) and the catalytic domain (151-313).

Cofactor binding domain

The cofactor-binding domain exhibits the typical Rossmann fold (β - α - β fold).²⁹ In all subunits the electron density for NAD⁺ was excellent (Fig. S2) and their average B values were lower than the B average for the protein chains (Table 2). The ADP moiety of NAD⁺ binds to the N-terminal β - α - β motif. Active site residues Gly⁷-Phe-Gly-Arg-Ile-Gly-Arg¹³ and Ile¹⁴⁵/Val-Ser-Asn/Gly-Ala-Ser-Cys-Thr-Thr-Asn-Cys¹⁵⁴/Ser are conserved in GAPDHs of various organisms (Fig. S1, S3). In

*Ct*GAPDH six residues (Arg10, Ile11, Asp33, Lys77, Thr119 and Asn314) directly contact NAD⁺ [Fig. 3(A)]. Main chain nitrogen atoms of Arg10 and Ile11 form hydrogen bonds to the pyrophosphate while side chain oxygen atoms of the conserved Asp33 interact with hydroxyl oxygen atoms of the adenosine ribose. The peptide oxygen atom of Lys77 forms a hydrogen bond with the adenine amino group. The corresponding residue in human GAPDH (hGAPDH, *IU8F*) Arg80 also exhibits a similar hydrogen bond.³⁰ Notably, this hydrogen bond was absent from the *6OK4* model. At the nicotinamide end of the dinucleotide, Thr119 is hydrogen bonded to the ribose and Asn314 forms a hydrogen bond with the amide oxygen of nicotinamide. Table S1 lists the hydrogen bonds between the protein and the co-factor.

Active site

The GAPDH catalytic domain is composed of a six-stranded β -sheet, three α -helices and two additional short helices, with catalytic cysteine (Cys150) and histidine (His177) residues positioned for reaction with the substrate. The overall structures of *Ct*GAPDH holo-form and *GBSGAPDH* ternary complex (*5JYA*) are similar (*rmsd* 0.95Å for tetramers), and the catalytic residues in these structures superpose well [Fig. 3(B)]. In *Ct*GAPDH the Cys150 sulfhydryl atom is at a distance of 3.5-3.6 Å from the carbonyl carbon (C1) atom of D-G3P (based on its position in *5JYA* subunit A). Residues that interact with the C3-phosphate are also conserved in *Ct*GAPDH (Ser149, Thr151 and Gly210). One water molecule is found at or near the predicted location for the O3P atom of the C3-phosphate group [Fig. 3(B)]. When compared with *5JYA*, the *Ct*GAPDH structure deviates in the helix-loop segment (residues 209-220). In *5JYA* two conserved residues,

Thr212 and Gly213, within this loop interact with the phosphate of the substrate. Divergence between these structures is also observed in a loop consisting of residues 122-126 and in another loop known as the S-loop.

The T-cell antigenic peptide is located with the S-loop

GAPDH structures feature a long loop called the S-loop. In the *Ct*GAPDH structure, the electron density for the S-loop (residues 179-200) is excellent. The average B value for these residues (12.96 \AA^2) in each subunit is lower than the B-average for the protein (15.7 \AA^2). Several residues in the S-loop are involved in inter-subunit interactions across the P and Q interfaces and thus in the assembly of the tetramer. Arg195 and Arg198 of subunit A form salt bridges with Asp294 and Asp283 of subunit B, respectively. Subunit A residues Asp187, Arg191 and Arg198 form hydrogen bonds with Arg13, Leu34, Tyr42 and Ser48 of subunit C, respectively (Fig. S4). The peptide nitrogen atom of Ala181 forms a water-mediated interaction with NAD^+ in the same subunit.

The MHC class II bound peptides purified from *Cm*-infected mice included a 15 residue peptide corresponding to *Cm* GAPDH residues 173-187 ((**MTTVHA**ATATQ**SVVD**), where the nine core residues are shown in bold).²¹ The equivalent peptide in *Ct*GAPDH is located at the major interface on a long β -strand and extends into the S-loop. Three peptide residues (Ala179, Ser184 and Val185, underscored) belonging to the S-loop are conserved in GAPDHs of *Ct* and *Cm* but different in other organisms (Fig. S5). Markos *et al.*³¹ noted that the sequence of the S-loop carries the distinct signature for enzymes of eubacterial and eukaryotic origin.³¹ Selection of the T-cell antigenic peptide within the S-loop is therefore highly interesting. The S-loop sequences of

GAPDHs of *Ct* and *Cm* exhibit some differences from the prokaryotic and eukaryotic proteins but cluster more closely with *E. coli* and eukaryotic GAPDHs (Table 3).

CtGAPDH structure reveals modified cysteine residues

The electron density for Cys63 and Cys287 indicated that these residues were chemically modified [Fig. 4(A)]. Based on the shape of the electron density and refinement parameters we predicted that Cys63 was nitrosylated (SNC) presumably within *E. coli* and/or in the crystals, and Cys287 was oxidized by β -mercaptoethanol (BME, from the buffers) to S,S-(2-hydroxyethyl)thiocysteine (CME). Mass spectrometric analysis of freshly purified *CtGAPDH* revealed the presence of several modified protein derivatives along with unmodified protein (Fig. S6). The doubly modified protein containing SNC63 and CME287 represented a minor peak (~36,380 Da, indicated with * in Fig. S6) while the mass for the two most abundant forms matched those of the BME oxidation product (~36,350 Da) and the unmodified protein (~36,274 Da). There were additional peaks of higher molecular masses. Similar modifications were observed in the structure determined from a second crystal (coordinates and structure factors deposited in PDB as 6X2E). Details of crystallization, data collection and refinement parameters for 6X2E are described in the Supplementary Materials and Table S2.

SNC and CME modifications have been observed in protein structures.^{32,33} In GAPDH sequences a cysteine residue is present at position 287 only in *Chlamydiae* and certain coccidia (Fig. S3). In *CtGAPDH* residue CME287 is in a hydrophobic pocket formed by Tyr273, Phe284, Tyr289, Val292 and Trp311 [Fig. 4(B)]. Notably, the electron density map for the published

*Ct*GAPDH structure (6OK4) shows additional density near the Cys287 sulfur atom (Fig. S7) even though different purification and crystallization conditions were used by Barrett *et al.*²⁸

The cysteine residue in position 63 is unique in *Chlamydiae* GAPDH and is located on the protein surface. Regulatory functions of endogenously S-nitrosylated cysteine residues in GAPDH have been reported.³⁴ While a consensus linear motif for cysteine nitrosylation has not been identified, interactions with aromatic and basic residues are suggested to render cysteine residues susceptible to S-nitrosylation.³⁵ In the *Ct*GAPDH structure, aromatic residues Phe59, Leu64, Val65 and Phe73 and basic residues Lys70 and His72 are within 5 Å of SNC63 [Fig. 4(C)].

Chemical modifications of cysteine residues of GAPDH influence various cellular processes.^{34,36} Although modifications in native *Ct*GAPDH has not been reported, our results suggest the presence of one or more reactive cysteine residues in the protein.

GAPDH structures feature regions of low sequence identity

Alignment of *Ct*GAPDH and human GAPDH (hGAPDH) sequences exhibits ~55% identity and 69% similarity. In two areas within the cofactor-binding domain (Region1: residues 18-41 and Region2: 52-91), and in one area (Region3: 248-273) in the catalytic domain, *Ct*GAPDH and hGAPDH are only 21-31% identical [Fig. 5(A)]. Among the residues that directly interact with NAD⁺, Lys77 and Thr119 are replaced by an arginine and a serine residue, respectively, in hGAPDH. Differences are also apparent near the adenine-binding pocket (within Region 1). In this area, the hGAPDH sequence has one amino acid insertion (Pro36), and Phe37 in hGAPDH replaces Leu34 [Fig. 5(B)]. Similarly, despite the high overall sequence identity between

*Ct*GAPDH and *GBS*GAPDH (~45%) in Region 2 they share only ~18% identity [Fig. 5(C)]. Pairwise sequence alignment using Needle/EMBOSS (<https://www.ebi.ac.uk/Tools/psa/>) reveals that compared to *GBS*GAPDH there is an insertion (²⁷⁰Asn-Ile-Met-Tyr²⁷³) in Region 3 of *Ct*GAPDH. Moreover, the characteristic extension of a two-stranded β -sheet exposed on some bacterial GAPDHs is absent from the *Ct*GAPDH structure.^{37,38} The regions of low sequence identity are mainly distributed on the GAPDH protein surface and may be involved in specific intermolecular interactions.

***Ct*GAPDH binds to plasminogen and plasmin**

Some bacterial GAPDHs are known to bind host extracellular matrix proteins but such interactions have not been reported for *Ct*GAPDH. We examined the binding of *Ct*GAPDH with hPlg and hPln using Biolayer interferometry (BLI). Our results show that *Ct*GAPDH binds to both proteins with similar affinity (Fig. S8). The values for the dissociation constant (K_D) measured in our experiments were 0.33 μ M ($R^2 = 0.988$; $X^2 = 1.388$) for hPlg and 0.14 μ M ($R^2 = 0.9988$; $X^2 = 1.505$) for hPln, respectively. The association and dissociation rate constants for hPlg interactions were 3.25×10^5 (0.28×10^5) $M^{-1}s^{-1}$ and 1.083×10^{-1} (0.036×10^{-1}) s^{-1} , respectively. The association and dissociation rate constants for hPln interactions were 3.673×10^3 (0.056×10^3) $M^{-1}s^{-1}$ and 5.294×10^{-4} (0.277×10^{-4}) s^{-1} , respectively.

The Plg binding sites on different GAPDHs are not well characterized. Plg contains five ‘Kringles’ domains (K1, K2, K3, K4 and K5) that are lysine-binding modules known to be important for receptor binding.³⁹ Moreau *et al.* identified three lysine residues (Lys304, Lys115

and Lys116) of *S. pneumoniae* GAPDH (*Sp*GAPDH) critical for binding to hPlg.³⁸ Among these, Lys304 is located at the edge of the extended β -sheet structure seen in some bacterial GAPDHs. The structurally equivalent residue in *Ct*GAPDH is Asp303. *Sp*GAPDH residues Lys115 and Lys116 are replaced by Lys114 and Arg115 in *Ct*GAPDH, which are located on the protein surface. *Ct*GAPDH has 76 lysine residues (19 per subunit) exposed on the tetramer surface.

To predict the possible binding modes, we performed protein-protein docking using two different programs, ClusPro⁴⁰ and Gramm-X⁴¹ with *Ct*GAPDH tetramer (*6WYC*) as receptor and hPlg monomer (*4DUR*)⁴² as ligand. From the top ten docking models predicted by each program we selected a total of 3 based on i) stable docked assembly (positive ΔG_{diss} calculated by PISA⁴³) value and ii) utilization of Kringle domain for binding: model1 (GrammX), and models2 and 3 (ClusPro) with ΔG_{diss} values of 9.3, 7.2 and 6.2 kcal/mol, respectively (Table S3). In models 1 and 2, hPlg domains K3 (residues 255-340) and K4 (355-440) dock onto adjacent subunits of the *Ct*GAPDH tetramer. In model 1, the K3 domain interacts with three *Ct*GAPDH subunits. The hPlg K3 inserts into the inter-subunit space near Lys192 of subunit C (Fig. S9). The K4 docking surface shows interactions with Lys225 (subunit C), which forms a salt bridge/hydrogen bond with Glu395 of hPlg. In addition, Lys223 of subunit C is also located near the K4 domain. In model2, the K4 of hPlg docks on to a similar surface as in model1 but the K3 domain does not show interaction with any lysine residue (Fig. S10). In model3 all hPlg residues except Arg312 (K3) that are involved in *Ct*GAPDH binding are located outside any Kringle domain. In this pose, Lys85 and Lys114 are ~7-8 Å away from the nearest residue in the K3 domain. However, Plg also binds to arginine

residues.⁴⁴ In all three binding poses discussed above the *Ct*GAPDH active site remains accessible. Hydrogen bonds and salt bridges between the receptor and ligand in the three models are listed in **Table S3**.

CONCLUSIONS

The presence of GAPDH in both life stages of *Ct* is intriguing considering the versatile functions of GAPDHs. To establish and survive its intracellular life *Ct* interacts with many host molecules. It is not known if *Ct*GAPDH is present on the bacterial surface. However, its ability to bind to hPIg and hPI_n suggests that if attached to the outer surface *Ct*GAPDH can serve as a ligand for interaction with host extracellular matrix proteins. High resolution crystal structure reveals structural differences in the active sites of *Ct*GAPDH and hGAPDH, and shows areas of low sequence identity on the tetramer surface. These regions may be involved in specific functions. Although GAPDH is an evolutionarily conserved protein with considerable homology across the species antibodies raised against bacterial GAPDH can be highly specific.⁴⁵ Our data indicate the presence of reactive cysteine residues that may modulate non-enzymatic cellular functions of *Ct*GAPDH.

MATERIALS AND METHODS

Expression and purification

Ct gapdh sequence was cloned into *Escherichia coli* expression vector pJ411 (DNA2.0). *Ct*GAPDH was expressed in *E. coli* BL21(DE3) cells in LB medium containing 100 µg/ml

ampicillin. At mid-log phase recombinant protein expression was induced by adding 0.4 mM isopropyl-thio- β -D-galactoside and the culture was grown ~20 hours at 22°C. All subsequent steps were performed at 4°C. *Ct*GAPDH was isolated from the bacterial extract using ammonium sulfate precipitation. The majority of *Ct*GAPDH was obtained in the pellet at 50-60% saturation. The pellet was suspended in a minimum volume of 20 mM HEPES, pH 7.5, 0.1 mM NaCl, 5 mM BME and fractionated on a Superdex 200 column (GE Healthcare) in the same buffer. Pooled fractions containing tetrameric *Ct*GAPDH were further purified on a DEAE Sephacel column (GE Healthcare) and eluted between 250-300 mM NaCl concentration in 20 mM Tris HCl, pH 8.0, 5 mM BME.

Enzyme activity and kinetics

The optimum pH for *Ct*GAPDH activity was determined by measuring initial reaction velocities in the pH range of 5-11 in a reaction buffer (50 mM triethanolamine, 50 mM sodium bisphosphate, 0.2 mM EDTA) using 0.5 μ g/mL *Ct*GAPDH, 0.6 mM NAD⁺ and 2 mM D-G3P. For each reaction the pH was adjusted after the addition of D-G3P and NAD⁺ prior to the addition of enzyme. Kinetic experiments were performed in a total volume of 1 mL with either saturating D-G3P (3 mM) and varying NAD⁺ (0.025-0.8 mM) or constant NAD⁺ (0.6 mM) and varying D-G3P (0.25-6 mM) in the reaction buffer (pH 9.0). Reactions (in triplicate) were initiated with the addition of 0.5 μ g *Ct*GAPDH. Reaction velocities were measured by monitoring the increase in absorbance (340 nm) for 1.3 min in a 1 cm path-length quartz cuvette in an HP 8542A Diode Array UV-Vis

spectrophotometer. The K_M and V_{max} parameters were determined by non-linear least square fitting of the (v_o) versus $[S]$ curve using GraphPad Prism (v7.0).

Crystallization and data collection

*Ct*GAPDH (30 mg/mL) was incubated at 4°C with 1 mM NAD^+ for 30 min and used for crystallization trials at 21°C using commercial screens. Crystals were obtained in PEG Suite I (Qiagen) condition #24 (25% PEG 2000 MME, 0.1 M Tris, pH 8.5) and flash frozen in the reservoir solution supplemented with 20% glycerol. X-ray diffraction data were collected on a Pilatus 6M hybrid pixel detector at the NE-CAT 24-ID-C beamline (Advanced Photon Source). Intensity data were integrated, merged and scaled with XDS⁴⁶ followed by Aimless in CCP4.⁴⁷ Data collection parameters are listed in Table 2.

Crystal structure determination and refinement

The structure of *Ct*GAPDH was solved by molecular replacement using Phaser⁴⁸ with a monomer of the *GBSGAPDH* (4QX6) as search model.³⁷ After refinement of the protein chains, one NAD^+ molecule was unambiguously placed in each subunit. Refinement was carried out by Refmac⁴⁹ and Phenix⁵⁰, and Coot⁵¹ was used for model building. Figures were created with PyMOL (Version 2.2.0; Schrödinger LLC). Refinement parameters are listed in Table 2. Clashscore and Molprobit score reported in Table 2 were calculated by using Molprobit (4.2).⁵² The coordinates and structure factors have been deposited in the Protein Data Bank under the code 6WYC.

Whole protein mass spectrometry

Purified CtGAPDH was diluted to a final concentration of 0.3 μM in water with 0.1% formic acid (v/v). The sample was chromatographically separated over a Phenomenex SecurityGuard Ultra C4 trap utilizing a gradient composed of SA (water with 0.1% [vol/vol] formic acid) and SB (acetonitrile with 0.1% [vol/vol] formic acid) on a Shimadzu SPD-20 series pump system. Detection was carried out on a Waters G2-Si Synapt mass spectrometer. Analysis was performed using the MaxEnt function in Waters MassLynx software.

Protein-protein interaction: Biolayer Interferometry

The BLItz biolayer interferometry instrument (Pall ForteBio) was used to measure the binding affinities between CtGAPDH and hPln or hPlg. The High Precision Streptavidin (SAX) biosensors were used to immobilize biotin-labeled hPln (Sigma, P1867) and hPlg (Sigma, P1517) via interaction with the Streptavidin. The amino groups of hPln and hPlg were labeled with biotin using EZ-Link NHs-PEG4-Biotin (Thermo Fisher Scientific) according to manufacturer's instructions. Titrations were performed using varying concentrations of CtGAPDH in the range of 0.15-0.57 μM for hPlg binding and 1.5-3.7 μM for hPln binding. The running buffer consisted of 1X PBS and 1X Kinetic buffer (Pall ForteBio). The composition of the Kinetic buffer was as follows: 10mM phosphate, 150 mM NaCl, 0.02% Tween 20, 0.05% sodium azide, 1 mg/mL BSA, pH 7.4.

ACKNOWLEDGEMENTS

We thank Dr. Peter Edward Prevelige, Jr. (UAB Microbiology Department) for assistance with mass spectroscopy data collection. This work was supported in part with funding from a Project Grant from the National Health and Medical Research Council (NHMRC) Australia (APP1129928) to GCU and DC. NE-CAT beamlines and the detector are supported by National Institutes of Health Grant Number: (P30 GM124165) and RR029205 at the APS (DE-AC02-06CH11357).

CONFLICT OF INTEREST

The authors declare that they have no conflict of interest with the content of this article.

REFERENCES

1. Skipp PJ, Hughes C, McKenna T, Edwards R, Langridge J, Thomson NR, Clarke IN (2016) Quantitative proteomics of the infectious and replicative forms of *Chlamydia trachomatis*. *PLoS One* 11:e0149011.
2. Dolat L, Valdivia RH (2019) A renewed tool kit to explore *Chlamydia* pathogenesis: from molecular genetics to new infection models. *F1000Res* 8:F1000 Faculty Rev-935.
3. Price MJ, Ades AE, De Angelis D, Welton NJ, Macleod J, Soldan K, Simms I, Turner K, Horner PJ (2013) Risk of pelvic inflammatory disease following *Chlamydia trachomatis* infection: analysis of prospective studies with a multistate model. *Am J Epidemiol* 178:484-492.
4. Kong FY, Hocking JS (2015) Treatment challenges for urogenital and anorectal *Chlamydia trachomatis*. *BMC Infect Dis* 15:293.
5. Phillips S, Quigley BL, Timms P (2019) Seventy years of *Chlamydia* vaccine research - limitations of the past and directions for the future. *Front Microbiol* 10:70.
6. Iliffe-Lee ER, McClarty G (1999) Glucose metabolism in *Chlamydia trachomatis*: the 'energy parasite' hypothesis revisited. *Mol Microbiol* 33:177-187.

- Accepted Article
7. Aronov AM, Verlinde CL, Hol WG, Gelb MH (1998) Selective tight binding inhibitors of trypanosomal glyceraldehyde-3-phosphate dehydrogenase via structure-based drug design. *J Med Chem* 41:4790-4799.
 8. Chauhan AS, Kumar M, Chaudhary S, Patidar A, Dhiman A, Sheokand N, Malhotra H, Raje CI, Raje M (2017) Moonlighting glycolytic protein glyceraldehyde-3-phosphate dehydrogenase (GAPDH): an evolutionarily conserved plasminogen receptor on mammalian cells. *FASEB J* 31:2638-2648.
 9. Pancholi V, Fischetti VA (1992) A major surface protein on group A streptococci is a glyceraldehyde-3-phosphate-dehydrogenase with multiple binding activity. *J Exp Med* 176:415-426.
 10. Crowe JD, Sievwright IK, Auld GC, Moore NR, Gow NA, Booth NA (2003) *Candida albicans* binds human plasminogen: identification of eight plasminogen-binding proteins. *Mol Microbiol* 47:1637-1651.
 11. Seifert KN, McArthur WP, Bleiweis AS, Brady LJ (2003) Characterization of group B streptococcal glyceraldehyde-3-phosphate dehydrogenase: surface localization, enzymatic activity, and protein-protein interactions. *Can J Microbiol* 49:350-356.
 12. Madureira P, Baptista M, Vieira M, Magalhaes V, Camelo A, Oliveira L, Ribeiro A, Tavares D, Trieu-Cuot P, Vilanova M, Ferreira P (2007) *Streptococcus agalactiae* GAPDH is a virulence-associated immunomodulatory protein. *J Immunol* 178:1379-1387.
 13. Matta SK, Agarwal S, Bhatnagar R (2010) Surface localized and extracellular Glyceraldehyde-3-phosphate dehydrogenase of *Bacillus anthracis* is a plasminogen binding protein. *Biochim Biophys Acta* 1804:2111-2120.
 14. Magalhaes V, Andrade EB, Alves J, Ribeiro A, Kim KS, Lima M, Trieu-Cuot P, Ferreira P (2013) Group B *Streptococcus* hijacks the host plasminogen system to promote brain endothelial cell invasion. *PLoS One* 8:e63244.
 15. Terao Y, Yamaguchi M, Hamada S, Kawabata S (2006) Multifunctional glyceraldehyde-3-phosphate dehydrogenase of *Streptococcus pyogenes* is essential for evasion from neutrophils. *J Biol Chem* 281:14215-14223.
 16. Terrasse R, Tacnet-Delorme P, Moriscot C, Perard J, Schoehn G, Vernet T, Thielens NM, Di Guilmi AM, Frachet P (2012) Human and pneumococcal cell surface glyceraldehyde-3-phosphate dehydrogenase (GAPDH) proteins are both ligands of human C1q protein. *J Biol Chem* 287:42620-42633.
 17. Lama A, Kucknoor A, Mundodi V, Alderete JF (2009) Glyceraldehyde-3-phosphate dehydrogenase is a surface-associated, fibronectin-binding protein of *Trichomonas vaginalis*. *Infect Immun* 77:2703-2711.
 18. Bergmann S, Rohde M, Hammerschmidt S (2004) Glyceraldehyde-3-phosphate dehydrogenase of *Streptococcus pneumoniae* is a surface-displayed plasminogen-binding protein. *Infect Immun* 72:2416-2419.

- Accepted Article
19. Jung DW, Kim WH, Seo S, Oh E, Yim SH, Ha HH, Chang YT, Williams DR (2014) Chemical targeting of GAPDH moonlighting function in cancer cells reveals its role in tubulin regulation. *Chem Biol* 21:1533-1545.
 20. Alves J, Madureira P, Baltazar MT, Barros L, Oliveira L, Dinis-Oliveira RJ, Andrade EB, Ribeiro A, Vieira LM, Trieu-Cuot P, Duarte JA, Carvalho F, Ferreira P (2015) A safe and stable neonatal vaccine targeting GAPDH confers protection against Group B Streptococcus infections in adult susceptible mice. *PLoS One* 10:e0144196.
 21. Karunakaran KP, Rey-Ladino J, Stoykov N, Berg K, Shen C, Jiang X, Gabel BR, Yu H, Foster LJ, Brunham RC (2008) Immunoproteomic discovery of novel T cell antigens from the obligate intracellular pathogen Chlamydia. *J Immunol* 180:2459-2465.
 22. Lambeir AM, Loiseau AM, Kuntz DA, Vellieux FM, Michels PA, Opperdoes FR (1991) The cytosolic and glycosomal glyceraldehyde-3-phosphate dehydrogenase from *Trypanosoma brucei*. Kinetic properties and comparison with homologous enzymes. *Eur J Biochem* 198:429-435.
 23. Penkler G, du Toit F, Adams W, Rautenbach M, Palm DC, van Niekerk DD, Snoep JL (2015) Construction and validation of a detailed kinetic model of glycolysis in *Plasmodium falciparum*. *FEBS J* 282:1481-1511.
 24. Cook WJ, Senkovich O, Chattopadhyay D (2009) An unexpected phosphate binding site in glyceraldehyde 3-phosphate dehydrogenase: crystal structures of apo, holo and ternary complex of *Cryptosporidium parvum* enzyme. *BMC Struct Biol* 9:9.
 25. Schmalhausen EV, Shumkov MS, Muronetz VI, Svedas VK (2019) Expression of glyceraldehyde-3-phosphate dehydrogenase from *M. tuberculosis* in *E. coli*. Purification and characteristics of the untagged recombinant enzyme. *Protein Expr Purif* 157:28-35.
 26. Michels S, Rogalska E, Branlant G (1996) Phosphate-binding sites in phosphorylating glyceraldehyde-3-phosphate dehydrogenase from *Bacillus stearothermophilus*. *Eur J Biochem* 235:641-647.
 27. Kim H, Feil IK, Verlinde CL, Petra PH, Hol WG (1995) Crystal structure of glycosomal glyceraldehyde-3-phosphate dehydrogenase from *Leishmania mexicana*: implications for structure-based drug design and a new position for the inorganic phosphate binding site. *Biochemistry* 34:14975-14986.
 28. Barrett KF, Dranow DM, Phan IQ, Michaels SA, Shaheen S, Navaluna ED, Craig JK, Tillery LM, Choi R, Edwards TE, Conrady DG, Abendroth J, Horanyi PS, Lorimer DD, Van Voorhis WC, Zhang Z, Barrett LK, Subramanian S, Staker B, Fan E, Myler PJ, Sogge OO, Hybiske K, Ojo KK (2020) Structures of glyceraldehyde 3-phosphate dehydrogenase in *Neisseria gonorrhoeae* and *Chlamydia trachomatis*. *Protein Sci* 29:768-778.
 29. Rao ST, Rossmann MG (1973) Comparison of super-secondary structures in proteins. *J Mol Biol* 76:241-256.
 30. Jenkins JL, Tanner JJ (2006) High-resolution structure of human D-glyceraldehyde-3-phosphate dehydrogenase. *Acta Cryst D* 62:290-301.

- Accepted Article
31. Markos A, Miretsky A, Muller M (1993) A glyceraldehyde-3-phosphate dehydrogenase with eubacterial features in the amitochondriate eukaryote, *Trichomonas vaginalis*. *J Mol Evol* 37:631-643.
 32. Chen YY, Chu HM, Pan KT, Teng CH, Wang DL, Wang AH, Khoo KH, Meng TC (2008) Cysteine S-nitrosylation protects protein-tyrosine phosphatase 1B against oxidation-induced permanent inactivation. *J Biol Chem* 283:35265-35272.
 33. Lau K, Podolec R, Chappuis R, Ulm R, Hothorn M (2019) Plant photoreceptors and their signaling components compete for COP1 binding via VP peptide motifs. *EMBO J* 38:e102140.
 34. Hara MR, Cascio MB, Sawa A (2006) GAPDH as a sensor of NO stress. *Biochim Biophys Acta* 1762:502-509.
 35. Hao G, Derakhshan B, Shi L, Campagne F, Gross SS (2006) SNOSID, a proteomic method for identification of cysteine S-nitrosylation sites in complex protein mixtures. *Proc Natl Acad Sci USA* 103:1012-1017.
 36. Hildebrandt T, Knuesting J, Berndt C, Morgan B, Scheibe R (2015) Cytosolic thiol switches regulating basic cellular functions: GAPDH as an information hub? *Biol Chem* 396:523-537.
 37. Schormann N, Ayres CA, Fry A, Green TJ, Banerjee S, Ulett GC, Chattopadhyay D (2016) Crystal structures of Group B *Streptococcus* glyceraldehyde-3-phosphate dehydrogenase: Apo-form, binary and ternary complexes. *PLoS One* 11:e0165917.
 38. Moreau C, Terrasse R, Thielens NM, Vernet T, Gaboriaud C, Di Guilmi AM (2017) Deciphering key residues involved in the virulence-promoting interactions between *Streptococcus pneumoniae* and human plasminogen. *J Biol Chem* 292:2217-2225.
 39. Miles LA, Lighvani S, Baik N, Parmer CM, Khaldoyanidi S, Mueller BM, Parmer RJ (2014) New insights into the role of Plg-RKT in macrophage recruitment. *Int Rev Cell Mol Biol* 309:259-302.
 40. Kozakov D, Hall DR, Xia B, Porter KA, Padhorny D, Yueh C, Beglov D, Vajda S (2017) The ClusPro web server for protein-protein docking. *Nat Protoc* 12:255-278.
 41. Tovchigrechko A, Vakser IA (2006) GRAMM-X public web server for protein-protein docking. *Nucleic Acids Res* 34:W310-314.
 42. Law RH, Caradoc-Davies T, Cowieson N, Horvath AJ, Quek AJ, Encarnacao JA, Steer D, Cowan A, Zhang Q, Lu BG, Pike RN, Smith AI, Coughlin PB, Whisstock JC (2012) The X-ray crystal structure of full-length human plasminogen. *Cell Rep* 1:185-190.
 43. Krissinel E, Henrick K (2007) Inference of macromolecular assemblies from crystalline state. *J Mol Biol* 372:774-797.
 44. Sanderson-Smith ML, Downton M, Ranson M, Walker MJ (2007) The plasminogen-binding group A streptococcal M protein-related protein Prp binds plasminogen via arginine and histidine residues. *J Bacteriol* 189:1435-1440.
 45. Madureira P, Andrade EB, Gama B, Oliveira L, Moreira S, Ribeiro A, Correia-Neves M, Trieu-Cuot P, Vilanova M, Ferreira P (2011) Inhibition of IL-10 production by maternal

antibodies against Group B Streptococcus GAPDH confers immunity to offspring by favoring neutrophil recruitment. *PLoS Pathog* 7:e1002363.

46. Kabsch W (2010) Xds. *Acta Cryst D*66:125-132.
47. Winn MD, Ballard CC, Cowtan KD, Dodson EJ, Emsley P, Evans PR, Keegan RM, Krissinel EB, Leslie AG, McCoy A, McNicholas SJ, Murshudov GN, Pannu NS, Potterton EA, Powell HR, Read RJ, Vagin A, Wilson KS (2011) Overview of the CCP4 suite and current developments. *Acta Cryst D*67:235-242.
48. McCoy AJ, Grosse-Kunstleve RW, Adams PD, Winn MD, Storoni LC, Read RJ (2007) Phaser crystallographic software. *J Appl Cryst* 40:658-674.
49. Murshudov GN, Vagin AA, Dodson EJ (1997) Refinement of macromolecular structures by the maximum-likelihood method. *Acta Cryst D*53:240-255.
50. Afonine PV, Grosse-Kunstleve RW, Echols N, Headd JJ, Moriarty NW, Mustyakimov M, Terwilliger TC, Urzhumtsev A, Zwart PH, Adams PD (2012) Towards automated crystallographic structure refinement with phenix.refine. *Acta Cryst D*68:352-367.
51. Emsley P, Lohkamp B, Scott WG, Cowtan K (2010) Features and development of Coot. *Acta Cryst D*66:486-501.
52. Chen VB, Arendall WB, 3rd, Headd JJ, Keedy DA, Immormino RM, Kapral GJ, Murray LW, Richardson JS, Richardson DC (2010) MolProbity: all-atom structure validation for macromolecular crystallography. *Acta Cryst D*66:12-21.

Table 1. Kinetic Parameters for CtGAPDH and GAPDHs of some other organisms.

| | K_M NAD ⁺ mM | K_M G3P mM | V_{max} μ M NADH min ⁻¹ mg ⁻¹ | Ref. |
|--------------------------------|---------------------------|---------------|---|-----------|
| <i>T. brucei</i> (glycosomal) | 0.45 (0.18)* | 0.15 (0.06) | 294 (59) | 22 |
| <i>T. brucei</i> (cytosolic) | 0.04 (0.02) | 0.17 (0.01) | 270 (60) | 22 |
| Human Erythrocyte | 0.05 (0.01) | 0.07 (0.01) | 69 (5) | 22 |
| Rabbit muscle | 0.06 (0.01) | 0.082 (0.009) | 73 (2) | 22 |
| Yeast | 0.090 (0.009) | 0.21 (0.03) | 99 (18) | 22 |
| <i>B. stearothermophilus</i> | 0.039 (0.006) | 0.09 (0.01) | 225 (6) | 22 |
| <i>B. stearothermophilus</i> † | 0.15 (0.03) | 0.80 (0.09) | 70 (6) | 27 |
| <i>C. trachomatis</i> | 0.139 (0.016) | 0.611 (0.089) | 49.6 (1.84) | This work |
| <i>P. falciparum</i> | 0.57 (0.06) | 0.9 (0.1) | 3.1 (0.2) | 23 |
| <i>C. parvum</i> | 0.032 (0.002) | 0.763 (0.043) | 72 (2) | 25 |
| Group A Strep | 0.156 | 1.33 | 19.48 | 9 |
| <i>M. tuberculosis</i> | 0.135 (0.05) | 0.58 (0.1) | 55 (5) | 26 |
| | | | | |

*Standard deviations are shown in parenthesis.

†Assays were performed at the optimum pH (8.9) for *B. stearothermophilus* GAPDH. The study in reference 22 was conducted at pH 7.6.

T. brucei: *Trypanosoma brucei*

B. stearothermophilus: *Bacillus stearothermophilus* (*Geobacillus stearothermophilus*)

C. trachomatis: *Chlamydia trachomatis*

P. falciparum: *Plasmodium falciparum*

C. parvum: *Cryptosporidium parvum*

Group A Strep: Group A *Streptococcus*

M. tuberculosis: *Mycobacterium tuberculosis*

Table 2. Data collection and refinement statistics for *CtGAPDH* (6WYC).

Data collection

| | |
|-------------------------------------|---------------------------------------|
| Space Group | P2 ₁ |
| Unit cell parameters [Å; °] 97.4 | a = 66.60, b = 104.05, c = 86.47; β = |
| Resolution [Å] | 66.17-1.50 (1.53-1.50)* |
| Unique reflections | 173217 (8596) |
| Completeness [%] | 93.2 (93.0) |
| Redundancy | 3.3 (3.3) |
| R _{merge} [%] | 7.6 (62.6) |
| R _{meas} [%] | 8.9 (74.2) |
| R _{pim} [%] | 4.5 (38.8) |
| I/σ(I) | 10.2 (1.9) |
| CC _{1/2} | 0.997 (0.681) |

Refinement

| | |
|----------------|------------------------|
| Resolution [Å] | 66.26-1.50 (1.54-1.50) |
|----------------|------------------------|

| | |
|-------------------------------------|------------------------|
| No. of unique reflections | 173177 (12748) |
| Completeness [%] | 92.9 (92.8) |
| R _{work} [%] | 17.0 (27.7) |
| R _{free} [%] | 18.9 (29.1) |
| Atoms (Protein, Ligands, Waters) | 10251, 176, 1230 |
| Wilson B [Å ²] | 12.3 |
| Average B-factors [Å ²] | |
| Overall, Protein, Ligands, Waters | 17.1, 15.7, 10.0, 29.3 |
| <i>Rmsd</i> bonds [Å] | 0.013 |
| <i>Rmsd</i> angles [°] | 1.69 |
| CC (Fo-Fc) | 0.96 |
| Ramachandran | |
| Favored, allowed, outlier (%) | 97, 2.7, 0.3 |
| Clash score† | 2.50 |
| Molprobrity score† | 1.21 |

*Numbers in the parenthesis are for the highest resolution shell.

†Clash score and Molprobrity score are calculated by using Molprobrity (4.2)⁵²

| | | | | | | | | | | | | | | | | | | | | | | | | | | | | | |
|-----|---|---|---|---|---|---|---|---|---|---|---|---|---|---|---|---|---|---|---|---|---|---|---|---|---|---|---|---|--|
| Bst | Y | T | N | D | Q | R | I | L | D | L | P | - | | | H | K | D | | | L | R | R | A | R | A | A | A | E | |
| Bsu | Y | T | N | D | Q | Q | I | L | D | L | P | - | | | H | K | D | | | Y | R | R | A | R | A | A | A | E | |
| Ta | Y | T | N | D | Q | R | L | L | D | L | P | - | | | H | K | D | | | L | R | R | A | R | A | A | A | I | |
| Tv | Y | T | N | D | Q | V | V | A | D | T | M | - | | | H | K | D | | | L | R | R | A | R | A | A | G | M | |
| Cg | Y | T | G | D | Q | R | L | H | D | A | P | - | | | H | R | D | | | L | R | R | A | R | A | A | A | V | |
| At | Y | T | G | D | Q | R | L | L | D | A | S | - | | | H | R | D | | | L | R | R | A | R | A | A | A | L | |
| Sp | T | T | G | D | Q | M | I | L | D | G | P | - | | | H | R | G | G | D | L | R | R | A | R | A | G | A | A | |
| Sag | Y | T | G | D | Q | M | I | L | D | G | P | - | | | H | R | G | G | D | L | R | R | A | R | A | G | A | A | |
| Sa | Y | T | G | D | Q | N | T | Q | D | A | P | - | | | H | R | K | G | D | K | R | R | A | R | A | A | A | E | |
| Clp | Y | T | N | D | Q | N | T | L | D | G | P | | | | H | R | K | G | D | F | R | R | A | R | A | A | A | V | |
| Ct | A | T | A | T | Q | S | V | V | D | G | P | S | | | R | K | D | | | W | R | G | G | R | G | A | F | Q | |
| Cm | A | T | A | T | Q | S | V | V | D | G | P | S | | | R | K | D | | | W | R | G | G | R | G | A | F | Q | |
| Ec | T | T | A | T | Q | K | T | V | D | G | P | S | | | H | K | D | | | W | R | G | G | R | G | A | S | Q | |
| Sc | L | T | A | T | Q | K | T | V | D | G | P | S | | | H | K | D | | | W | R | G | G | R | T | A | S | G | |
| Tc | T | T | A | T | Q | K | T | V | D | G | P | S | | | Q | K | D | | | W | R | G | G | R | G | A | A | Q | |
| Tb | T | T | A | T | Q | K | T | V | D | G | P | S | | | Q | K | D | | | W | R | G | G | R | G | A | A | Q | |
| Eh | T | T | A | T | Q | K | T | V | D | G | P | S | | | G | K | D | | | W | R | A | G | R | C | A | C | A | |
| Ce | V | T | A | T | Q | K | T | V | D | G | P | S | | | G | K | L | | | W | R | D | G | R | G | A | G | Q | |
| Hs | I | T | A | T | Q | K | T | V | D | G | P | S | | | G | K | L | | | W | R | D | G | R | G | A | L | Q | |
| Mm | I | T | A | T | Q | K | T | V | D | G | P | S | | | G | K | L | | | W | R | D | G | R | G | A | A | Q | |
| Rn | I | T | A | T | Q | K | T | V | D | G | P | S | | | G | K | L | | | W | R | D | G | R | G | A | A | Q | |
| Pf | S | T | A | N | Q | L | V | V | D | G | P | S | K | G | G | K | D | | | W | R | A | G | R | C | A | L | S | |
| Cp | L | T | A | N | Q | L | T | V | D | G | P | S | K | G | G | K | D | | | W | R | A | G | R | C | A | G | N | |
| Tg | M | T | A | N | Q | L | T | V | D | G | P | S | K | G | G | K | D | | | W | R | A | G | R | S | A | G | V | |
| | | | | | | | | | | | | * | | | | | | | | * | | | | | | | | | |
| | | | | | | | | | | | | | | | | | | | | | | | | | | | | | |

Table 3. S-loop sequences in GAPDHs.

Bst: *Bacillus stearothermophilus* (*Geobacillus stearothermophilus*)

Bsu: *Bacillus subtilis*

Ta: *Thermus aquaticus*

Tv: *Trichomonas vaginalis*

Cg: *Corynebacterium glutamicum*

At: *Arabidopsis thaliana*

Sp: *Streptococcus pneumoniae*

Sag: *Streptococcus agalactiae* (GBS)

Sa: *Staphylococcus aureus*

Clp: *Clostridium pasteurianum*

Ct: *Chlamydia trachomatis*

Cm: *Chlamydia muridarum*
Ec: *Escherichia coli* (Gap A)
Sc: *Saccharomyces cerevisiae* (yeast)
Tc: *Trypanosoma cruzi*
Tb: *Trypanosoma brucei* (cytoplasmic)
Eh: *Entamoeba histolytica*
Ce: *Caenorhabditis elegans*
Hs: *Homo sapiens* (Human)
Mm: *Mus musculus* (Mouse)
Rn: *Rattus norvegicus* (Rat)
Pf: *Plasmodium falciparum*
Cp: *Cryptosporidium parvum*
Tg: *Toxoplasma gondii*

*Signature residues for eukaryotic GAPDHs are shaded in *Ct*GAPDH and *Cm*GAPDH S-loop sequences.

Chlamydiae specific residues Ala179, Ser184 and Val185 in the T-cell antigenic peptide are underlined. These residues are also underlined in Figure S3.

Figure Legends

Figure 1. Determination of pH optimum and kinetic parameters of *Ct*GAPDH enzyme activity.

- A. *Ct*GAPDH activity is shown at different pH. Initial reaction velocity (v_0) was measured.
- B. K_M and V_{max} for NAD^+ were determined from M-M plot. Assays were done in triplicate.
- C. K_M and V_{max} for D-G3P were determined from M-M plot. Assays were done in triplicate.

Figure 2. Structure of *Ct*GAPDH monomer and the assembly into dimers and tetramer.

- A. Cartoon drawing showing the tetrameric assembly of *Ct*GAPDH. NAD^+ is shown in stick model. Major interface axes P and Q are labeled. S-loop is colored fire brick.
- B. Subunits A, B and C, D form dimers. The AB dimer is shown with a close-up view of the major interface highlighted in green color on subunit A.
- C. Subunits A and C assemble across the Q-axis. Interface area on subunit A is shown in magenta color. The S-loop in subunit C is shown in fire brick color.
- D. The catalytic domain and the NAD^+ -binding domain in subunit A are colored yellow and light orange, respectively. Dimer interface area is shown in green. The S-loop is in fire brick color. The S-loop is also part of the second largest interface. Areas with strictly conserved residues (7-13 and 145-154) near the NAD^+ -binding pocket are shown in magenta color. NAD^+ is shown in stick model.

Figure 3. Interactions between NAD^+ and *Ct*GAPDH, and comparison of active sites in the binary and ternary complex.

- A. Interactions between *Ct*GAPDH (subunit A) residues and NAD⁺. *Ct*GAPDH residues (C: yellow) and NAD⁺ (C: green) are shown in stick models. Hydrogen bonding distances (Å) are shown.
- B. Superposition of subunits A of *Ct*GAPDH and *GBSGAPDH* ternary complex (*5JYA*). NAD⁺ and the substrate in *5JYA*, and the catalytic residues Cys150 and His177 in *Ct*GAPDH are in stick model (C: wheat color). The distance between Cys150Sγ and the C1 atom of the substrate is 3.6 Å, and between Cys150Sγ and His177Nε it is 3.3 Å. The catalytic residues of *5JYA* are also shown in stick model (C: slate color). The catalytic cysteine was mutated to serine in *5JYA*. Areas where the conformations differ significantly are shown in dark blue on the *GBSGAPDH* structures and the *Ct*GAPDH residues bordering the divergent areas are labeled. One water molecule (W177 shown as magenta sphere) is found at or near the site for the O3P atom of the substrate.

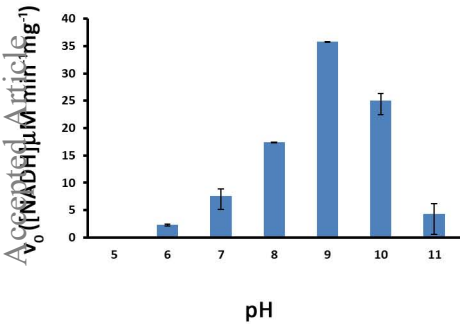
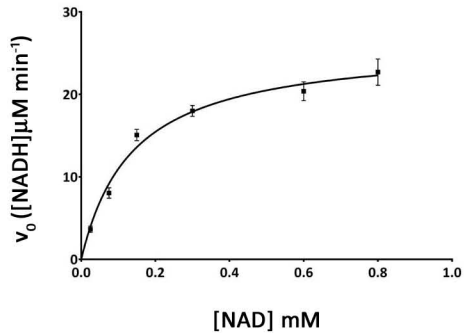
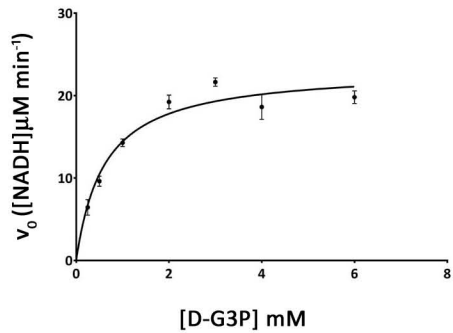
Figure 4. Electron density for the modified residues CME287 and SNC63, and their environment in *Ct*GAPDH crystal structure.

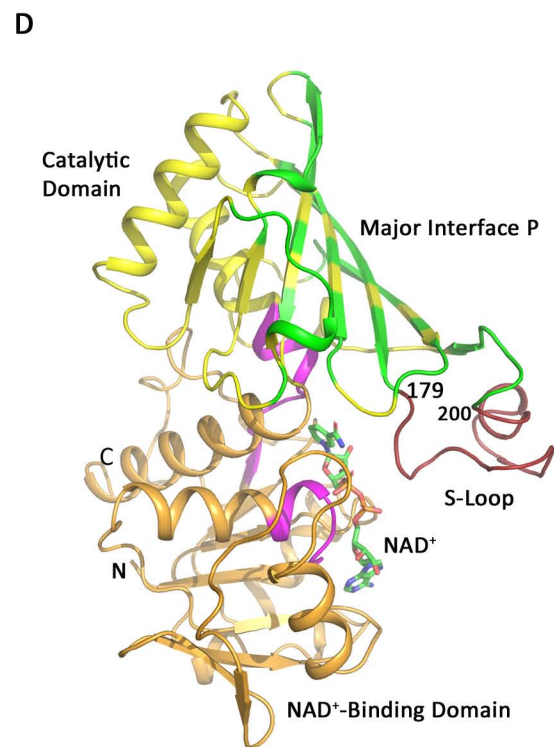
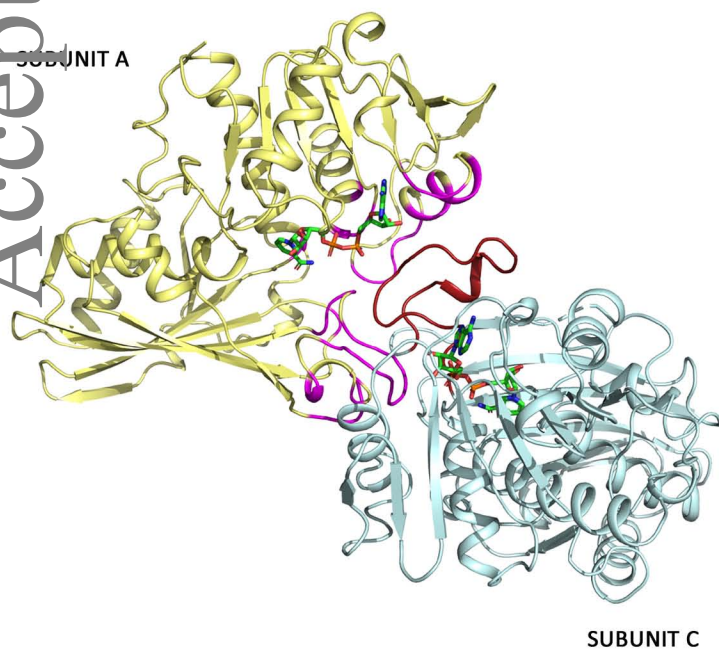
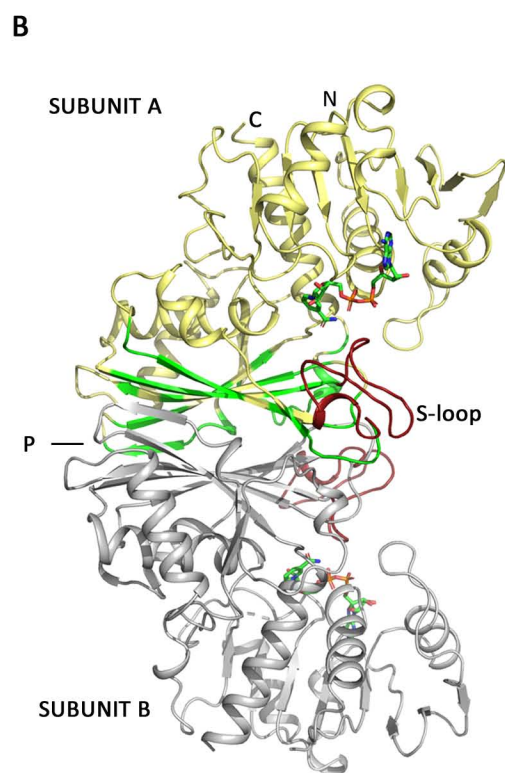
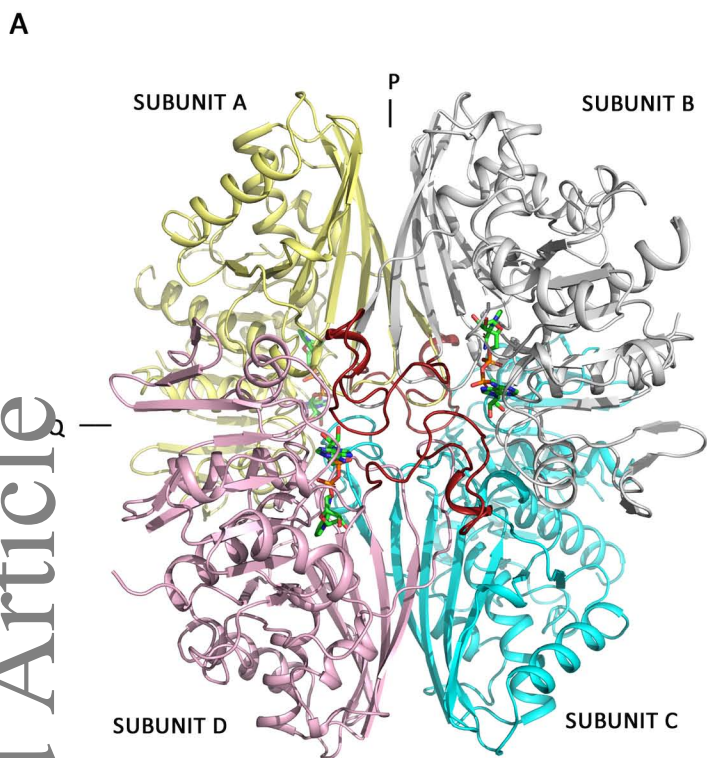
- A. Fo-Fc omit maps (mesh in light pink contoured at 3σ) for CME287 (upper panel) and SNC63 (lower panel). The residues are shown in stick model (C: white, N: blue, O: red, P: yellow).
- B. Aromatic and hydrophobic residues surrounding CME287 (C: green) are shown in stick model (C: yellow).

- C. Stereo diagram showing aromatic and basic residues within 5 Å of SNC63 (stick model, C: yellow).

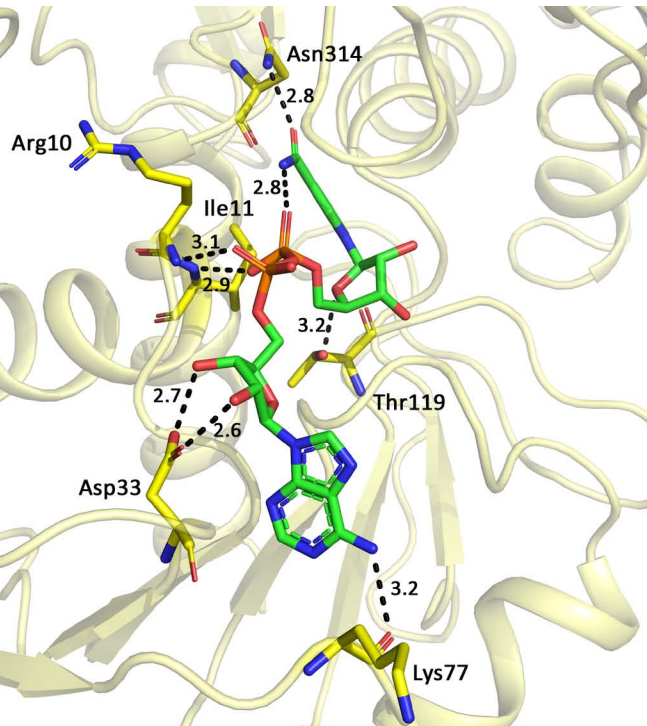
Figure 5. Comparison of different areas where *Ct*GAPDH sequence diverges from human and GBS GAPDH.

- A. Cartoon drawing showing superposition of subunit A of *Ct*GAPDH (light yellow) and hGAPDH (*IU8F* subunit O, light pink). Regions where the sequence identities are low are marked and shown in purple blue, slate and marine color. Comparison of these regions in the sequences for *Ct* and human (Hs) GAPDHs are shown. NAD⁺ is shown in stick model (C: green).
- B. Close-up view of the adenine binding pocket. Residues in hGAPDH (C: orange), *Ct*GAPDH (C: yellow) and NAD⁺ (C: green) are shown in stick models.
- C. Superposition of subunit A of *Ct*GAPDH (light yellow) and *GBSGAPDH* (*5JYA* subunit A, grey). Regions 2 and 3 where the sequence identities are low are marked and shown in slate and marine color. Comparison of these regions in the sequences for *Ct* and *GBSGAPDH*s are shown. NAD⁺ is shown in stick model (C: green).

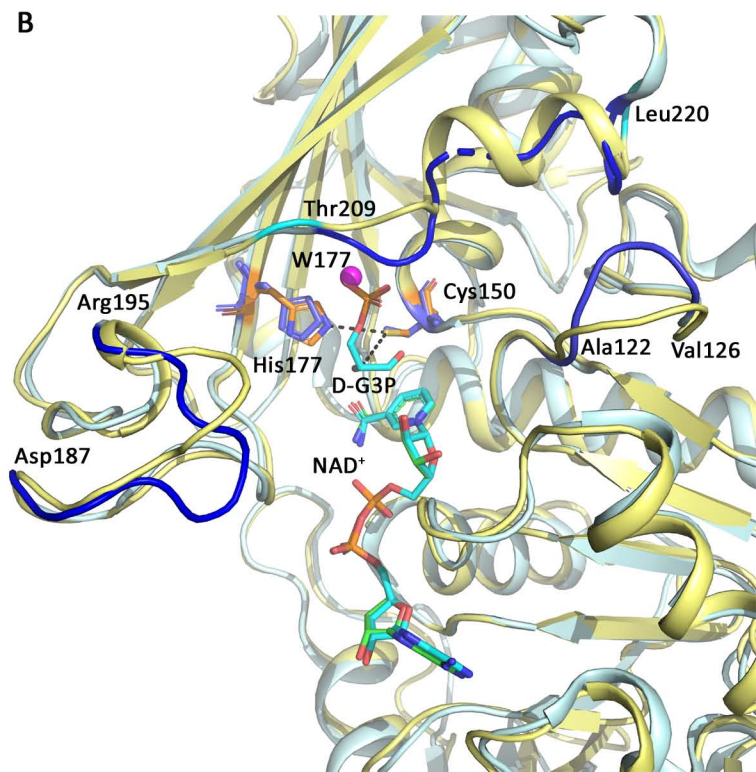
A**B****C**



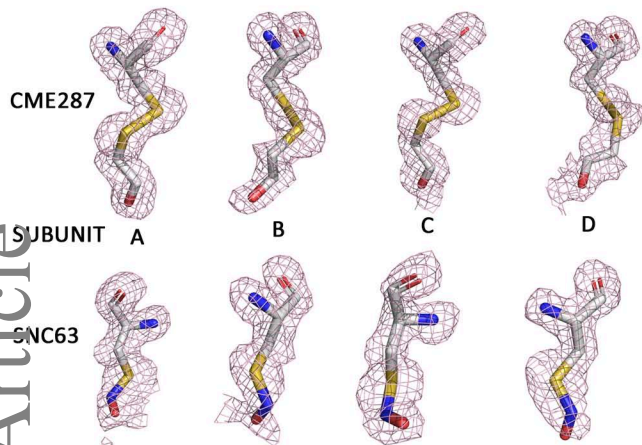
A



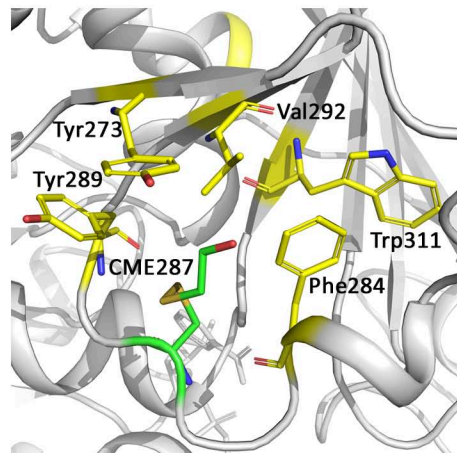
B



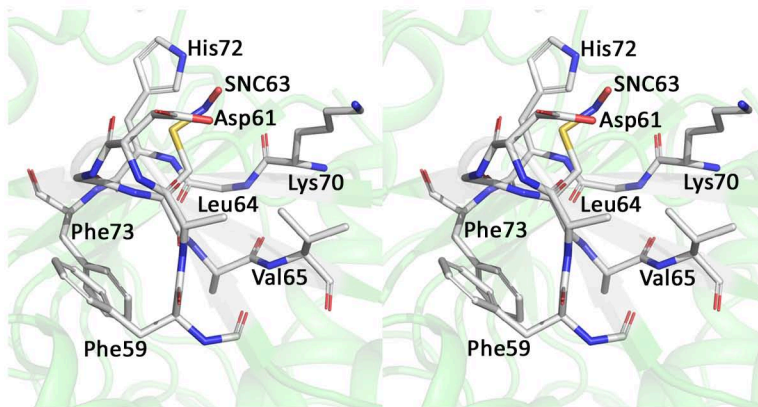
A



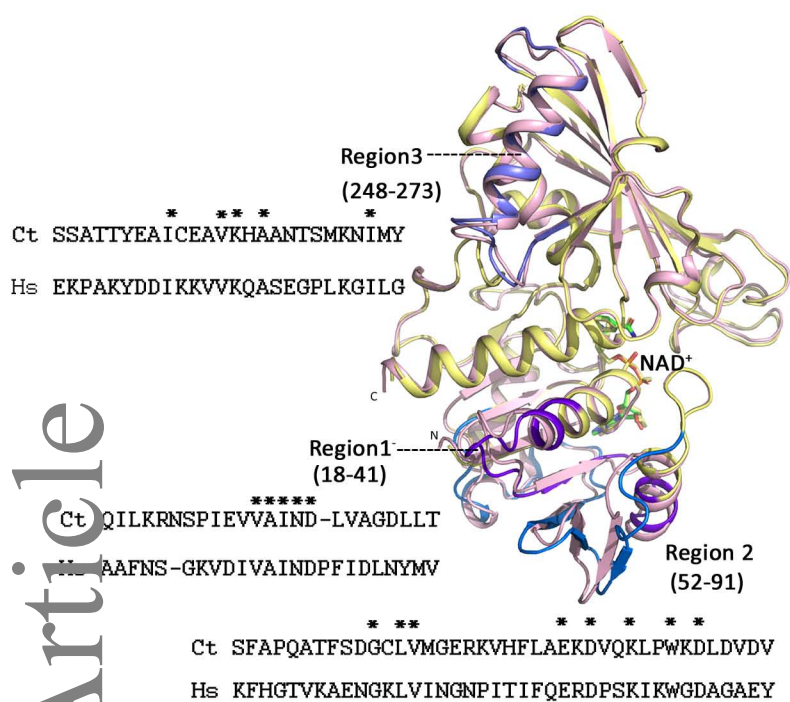
B



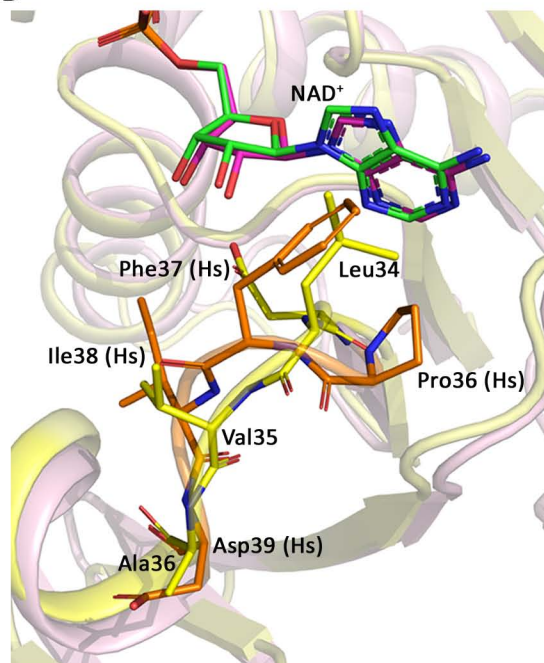
C



A



B



C

